NUMERICAL VERIFICATION OF DELTA SHOCK WAVES FOR PRESSURELESS GAS DYNAMICS

NATAŠA KREJIĆ, TANJA KRUNIĆ, MARKO NEDELJKOV

1. Introduction

Consider the Riemann problem for a pressureless gas dynamic model given by the system

$$\begin{aligned} u_t + (uv)_x &= 0 \\ (uv)_t + (uv^2)_x &= 0, \end{aligned} \tag{1}$$

and the initial data

$$u(x,0) = \begin{cases} u_l, x < 0 \\ u_r, x > 0 \end{cases}, \; v(x,0) = \begin{cases} v_l, x < 0 \\ v_r, x > 0 \end{cases}, \tag{2}$$

where u and v denote density and velocity, respectively.

The two eigenvalues of this system are equal, $\lambda_1 = \lambda_2 = v$ and the system is weakly hyperbolic. It has two types of solution depending on the initial conditions v_l and v_r. If $v_l \leq v_r$ then the system has a bounded weak entropy solution that is a combination of contact discontinuities and vacuum states ($u \equiv 0$). In the second case, when $v_l > v_r$ a delta shock wave solution exists, see [1], [16].

The subject of the present paper is theoretical analysis and numerical verification of delta shock wave existence for (1). Therefore we will consider only the case $v_l > v_r$. In this case the solution does not contain the vacuum state and we can transform the system into the evolutionary form

$$\begin{aligned} u_t + w_t &= 0 \\ w_t + (w^2/u)_x &= 0, \end{aligned} \tag{3}$$

introducing the new variable $w = uv$. The initial data is now given by

$$u(x,0) = \begin{cases} u_l, x < 0 \\ u_r, x > 0 \end{cases}, \; w(x,0) = \begin{cases} w_l = u_l v_l, x < 0 \\ w_r = u_r v_r, x > 0 \end{cases}.$$

There are two possible approaches to theoretical analysis of the considered problem. The measure theoretic solution to (1)-(2) constructed in a number of papers, for example [5] or [16], has a distributional limit given by

$$\begin{aligned} U(x,t) &\approx \begin{cases} u_l, x < ct \\ u_{r,} \; x > ct \end{cases} + (v_l - v_r)\sqrt{u_l u_r}\, t\delta(x - ct), \\ V(x,t) &\approx \begin{cases} v_l, x < ct \\ v_r, x > ct \end{cases}. \end{aligned}$$

The second possibility, which will be presented here, is to give a solution using generalized function space obtained from nets of smooth functions representing the

Department for Mathematics and Informatics, University of Novi Sad, Novi Sad, Trg Dositeja Obradovića 4, 21000 Novi Sad, Serbia, e-mail:natasak@uns.ns.ac.yu.

so-called generalized functions. Spaces of that type are already successfully used in numerics for PDE's. One can see [2] for some other examples. The particular version of Colombeau generalized functions, $\mathcal{G}_g(\mathbb{R}^2_+)$, used in the present paper is defined in [12]. Therefore we will solve Riemann problem for system (3) in the case $w_l/u_l > w_r/u_r$ using the above mentioned space of generalized functions. The obtained solution can be interpreted as a net of smooth functions possessing the distributional limit which contains the delta function. Further more the solution satisfies the admissibility condition for delta shock waves given by

$$\lambda_2(u_l, v_l) \geq \lambda_1(u_l, v_l) \geq c \geq \lambda_2(u_r, v_r) \geq \lambda_1(u_r, v_r).$$

The waves which satisfy the above condition are said to be overcompressive.

We will also present one numerical procedure that generates a solution in a large time interval and therefore gives a reasonable verification of theoretical results. The numerical solutions will be obtained for the system (1) and its perturbation

$$\begin{aligned} u_t + w_t &= 0 \\ w_t + (w^2/u + \mu u^\gamma)_x &= 0, \end{aligned} \tag{4}$$

where $1 < \gamma < 3$, $w_l/u_l > w_r/u_r$. Such perturbation is introduced in order to get strictly hyperbolic system. The perturbed system (4) is called isentropic gas dynamics model. We take γ to be constant or coupled with μ in such a way that $\gamma = \gamma(\mu) \to 1$ as $\mu \to 0$. Contrary to a viscosity approximation when a perturbed system is parabolic or mixed hyperbolic-parabolic, system (4) is hyperbolic so its Riemann problem can be solved by a combination of the usual elementary wave solutions.

In all three cases, the original problem and two different perturbations, the obtained results are mutually consistent and also consistent with generalized solution. Another interpretation of such result is that the numerical procedure used in this paper is robust enough to be applied to weakly hyperbolic problems.

There is a large class of numerical methods dealing with conservation laws. Roughly speaking, one can consider methods on fixed or moving meshes. As discontinuities propagate in time, the solution at a spatial point can change very rapidly and therefore fixed spatial mesh requires extremely small time step. On the other hand there is no justification for small time steps in smooth regions. That is why a nonuniform mesh with reasonably large spatial step in smooth regions and small step in discontinuity regions should be more efficient for this type of problems. As shocks travel in time, mesh should also be able to adjust in time so that points remain concentrated near discontinuities, thus maintaining a balance between computational costs and accuracy. Time adaptation can be done by static re-griding technique, or it can be based on dynamic refinement in which the mesh equation is explicitly derived. Based on the equidistribution principle, which attempts to distribute some measure of solution error over the spatial domain, dynamic refinement naturally generates concentration of mesh points in the regions of discontinuity. This technique leads to the coupled problem consisting of mesh equation based on monitor function and physical PDE, see [4] or [14].

High resolution finite volume methods are employed to solve the physical PDE. One of them is the wave propagation method introduced by LeVeque in [8] and implemented in the software package CLAWPACK [7]. The method is based on Godunov's scheme and Roe's solvers with addition of high resolution terms. One of the implementations of this method, coupled with dynamic refinement of mesh with fixed number of spatial points is presented in [14]. That algorithm, with the necessary adjustment to the specific problem we consider here, will serve as a base for our experiments.

Delta shock waves can be obtained using the following procedure. The first step is the smoothing of initial data (2) over some finite interval where a small parameter $\varepsilon > 0$ denotes the smoothing width. The second step is to find a smooth approximate solution depending on the given perturbation term to the Riemann problem. Interpretation of the solution can be given in the framework of Colombeau generalized functions algebras, like in [10] as already explained i.e solutions are considered as nets of smooth functions depending on a parameter ε with equality substituted by the distributional convergence as ε tends to zero.

Due to the specific nature of the delta shock waves (they contain δ-functions) it is not possible to follow the solution to (1) numerically in a large time interval. Therefore we will follow the solution only until a time point T where the delta shock is clearly formed.

The situation is different for the perturbed system (4) even for a small value of a perturbation coefficient μ. The solution is a combination of two shock waves in the case $w_l/u_l > w_r/u_r$, and we can follow the numerical solution for quite a long time.

The basic numerical algorithm will be the one presented in [14], with some adaptation to the specific problem we consider. First of all we apply the smoothing technique to initial data in order to avoid non-physical oscillations. The original problem (1) is modified by introducing the perturbation term shown in [4]. The monitor function used to distribute the mesh points is based on the arclength function with a parameter that prevents too many points in the shock regions but allows enough points in these regions. Furthermore the mesh is moving in spatial domain with time in order to follow the waves. These parameters (smoothing, perturbation, mesh parameter and spatial movement of the mesh) have a great influence on performance of the method and therefore need careful adjustment. Several properties of delta shock waves are exploited in order to check the relevance of obtained numerical solution.

This paper is organized as follows. Section 2 deals with theoretical analysis and establishes the existence of overcompressive delta shock wave solution in the framework of Colombeua generalized functions. The numerical algorithm is presented in Section 3. The algorithm is basically the one presented in [14]. Section 4 explains the criteria for evaluation of numerical results and two different perturbation used to get hyperbolic system. Numerical results are presented in Section 5.

2. Generalized solution

We shall briefly repeat some definitions of Colombeau algebra given in [12] and [10]. Denote $\mathbb{R}^2_+ := \mathbb{R} \times (0,\infty)$, $\overline{\mathbb{R}^2_+} := \mathbb{R} \times [0,\infty)$ and let $C^\infty_b(\Omega)$ be the algebra of smooth functions on Ω bounded together with all their derivatives. Let $C^\infty_{\overline{b}}(\mathbb{R}^2_+)$ be a set of all functions $u \in C^\infty(\mathbb{R}^2_+)$ satisfying $u|_{\mathbb{R}\times(0,T)} \in C^\infty_b(\mathbb{R} \times (0,T))$ for every $T > 0$. Let us remark that every element of $C^\infty_b(\mathbb{R}^2_+)$ has a smooth extension up to the line $\{t = 0\}$, i.e. $C^\infty_b(\mathbb{R}^2_+) = C^\infty_b(\overline{\mathbb{R}^2_+})$. This is also true for $C^\infty_{\overline{b}}(\mathbb{R}^2_+)$.

Definition 1. $\mathcal{E}_{M,g}(\mathbb{R}^2_+)$ is the set of all mappings $G : (0,1) \times \mathbb{R}^2_+ \to \mathbb{R}$, $(\varepsilon, x, t) \mapsto G_\varepsilon(x,t)$, where for every $\varepsilon \in (0,1)$, $G_\varepsilon \in C^\infty_{\overline{b}}(\mathbb{R}^2_+)$ satisfies:

For every $(\alpha,\beta)\in\mathbb{N}_0^2$ and $T>0$, there exists $N\in\mathbb{N}$ such that

$$\sup_{(x,t)\in\mathbb{R}\times(0,T)}|\partial_x^\alpha\partial_t^\beta G_\varepsilon(x,t)|=(\varepsilon^{-N}),\ \text{ as } \varepsilon\to 0.$$

$\mathcal{E}_{M,g}(\mathbb{R}^2_+)$ is an multiplicative differential algebra, i.e. a ring of functions with the usual operations of addition and multiplication, and differentiation which satisfies Leibnitz rule.

$\mathcal{N}_g(\mathbb{R}^2_+)$ is the set of all $G\in\mathcal{E}_{M,g}(\mathbb{R}^2_+)$, satisfying:
For every $(\alpha,\beta)\in\mathbb{N}_0^2$, $a\in\mathbb{R}$ and $T>0$

$$\sup_{(x,t)\in\mathbb{R}\times(0,T)}|\partial_x^\alpha\partial_t^\beta G_\varepsilon(x,t)|=\mathcal{O}(\varepsilon^{a}),\ \text{ as } \varepsilon\to 0.$$

□

Clearly, $\mathcal{N}_g(\mathbb{R}^2_+)$ is an ideal of the multiplicative differential algebra $\mathcal{E}_{M,g}(\mathbb{R}^2_+)$, i.e. if $G_\varepsilon\in\mathcal{N}_g(\mathbb{R}^2_+)$ and $H_\varepsilon\in\mathcal{E}_{M,g}(\mathbb{R}^2_+)$, then $G_\varepsilon H_\varepsilon\in\mathcal{N}_g(\mathbb{R}^2_+)$.

Definition 2. The multiplicative differential algebra $\mathcal{G}_g(\mathbb{R}^2_+)$ of generalized functions is defined by $\mathcal{G}_g(\mathbb{R}^2_+)=\mathcal{E}_{M,g}(\mathbb{R}^2_+)/_g(\mathbb{R}^2_+)$. All operations in $\mathcal{G}_g(\mathbb{R}^2_+)$ are defined by the corresponding ones in $\mathcal{E}_{M,g}(\mathbb{R}^2_+)$. □

If $C_b^\infty(\mathbb{R})$ is used instead of $C_b^\infty(\mathbb{R}^2_+)$ (i.e.$t=const=0$), then one obtains $\mathcal{E}_{M,g}(\mathbb{R})$, $\mathcal{N}_g(\mathbb{R})$, and consequently, the space of generalized functions on a real line, $\mathcal{G}_g(\mathbb{R})$.

In the sequel, G denotes an element (equivalence class) in $\mathcal{G}_g(\Omega)$ defined by its representative $G_\varepsilon\in\mathcal{E}_{M,g}(\Omega)$.

Since $C_{\overline{b}}^\infty(\mathbb{R}^2_+)=C_{\overline{b}}^\infty(\overline{\mathbb{R}^2_+})$, one can define the restriction of a generalized function to the line $\{t=0\}$ in the following way.

For a given $G\in\mathcal{G}_g(\mathbb{R}^2_+)$, its restriction $G|_{t=0}\in\mathcal{G}_g(\mathbb{R})$ is the class determined by a function $G_\varepsilon(x,0)\in\mathcal{E}_{M,g}(\mathbb{R})$. In the same way as above, $G(x-ct)\in\mathcal{G}_g(\mathbb{R})$ is defined by $G_\varepsilon(x-ct)\in\mathcal{E}_{M,g}(\mathbb{R})$.

If $G\in\mathcal{G}_g$ and $f\in C^\infty(\mathbb{R})$ are polynomially bounded together with all its derivatives, then one can easily show that the composition $f(G)$, defined by a representative $f(G_\varepsilon)$, $G\in\mathcal{G}_g$ makes sense. It means that $f(G_\varepsilon)\in\mathcal{E}_{M,g}$ if $G_\varepsilon\in\mathcal{E}_{M,g}$, and $f(G_\varepsilon)-f(H_\varepsilon)\in\mathcal{N}_g$ if $G_\varepsilon-H_\varepsilon\in\mathcal{N}_g$.

The equality in the space of the generalized functions $\mathcal{G}_g$ is too strong for our purpose (see [11] for some nice examples), so we need to define a weaker relation, the so-called association.

Definition 3. A generalized function $G\in\mathcal{G}_g(\Omega)$ is said to be *associated with* $u\in\mathcal{D}'(\Omega)$, $G\approx u$, if for some (and hence every) representative G_ε of G, $G_\varepsilon\to u$ in $\mathcal{D}'(\Omega)$ as $\varepsilon\to 0$. Two generalized functions G and H are said to be associated, $G\approx H$, if $G-H\approx 0$. The rate of convergence in $\mathcal{D}'$ with respect to ε is called the order of association. □

A generalized function G is said to be *of a bounded type* if

$$\sup_{(x,t)\in\mathbb{R}\times(0,T)}|G_\varepsilon(x,t)|=\mathcal{O}(1) \text{ as } \varepsilon\to 0,$$

for every $T>0$.

$G\in\mathcal{G}_g$ is a positive generalized function if there exists its representative G_ε and a real $a>0$ such that $G_\varepsilon(x,t)\geq a$, for every $(x,t)\in\mathbb{R}^2_+$. This condition on a representative also means that $G\geq a$.

Let $u \in \mathcal{D}'_{L^\infty}(\mathbb{R})$. Let $\mathcal{A}_0$ be the set of all functions $\phi \in C_0^\infty(\mathbb{R})$ satisfying $\phi(x) \geq 0$, $x \in \mathbb{R}$, $\int \phi(x)dx = 1$ and $\operatorname{supp}\phi \subset [-1,1]$, i.e.

$$\mathcal{A}_0 = \{\phi \in C_0^\infty : (\forall x \in \mathbb{R})\phi(x) \geq 0, \int \phi(x)dx = 1, \operatorname{supp}\phi \subset [-1,1]\}.$$

Let $\phi_\varepsilon(x) = \varepsilon^{-1}\phi(x/\varepsilon)$, $x \in \mathbb{R}$. Then

$$\iota_\phi : u \mapsto u * \phi_\varepsilon/\mathcal{N}_g,$$

where $u * \phi_\varepsilon/\mathcal{N}_g$ denotes the equivalence class with respect to the ideal $\mathcal{N}_g$, defines a mapping of $\mathcal{D}'_{L^\infty}(\mathbb{R})$ into $\mathcal{G}_g(\mathbb{R})$, where $*$ denotes the usual convolution in $\mathcal{D}'$. It is clear that ι_ϕ commutes with the derivation, i.e.

$$\partial_x \iota_\phi(u) = \iota_\phi(\partial_x u).$$

Definition 4. (a) $G \in \mathcal{G}_g(\mathbb{R})$ is said to be *a generalized step function* with value (y_0, y_1) if it is of bounded type and

$$G_\varepsilon(y) = \begin{cases} y_0, & y < -\varepsilon \\ y_1, & y > \varepsilon \end{cases}$$

Denote $[G] := y_1 - y_0$.

(b) $D \in \mathcal{G}_g(\mathbb{R})$ is said to be *generalized delta function* (δ*-function*, for short) if its representatives are nonnegative functions supported in $[-1,1]$ such that $\int D_\varepsilon(y)dy = 1$. $\square$

Suppose that the initial data are given by

$$u|_{t=T} = \begin{cases} u_0, & x < X \\ u_1, & x > X \end{cases} \quad v|_{t=T} = \begin{cases} v_0, & x < X \\ v_1, & x > X. \end{cases}$$

Definition 5. *Delta shock wave* is an associated solution to (3) of the form

$$\begin{aligned} u(x,t) &= G(x-ct) + s_1(t)D(x-ct) \\ w(x,t) &= H(x-ct) + s_2(t)D(x-ct), \end{aligned} \tag{5}$$

where

(i) $c \in \mathbb{R}$ is the speed of the wave,
(ii) $s_i(t)$, $t \geq 0$ are smooth functions, $s_i(0) = 0$, $i = 1, 2$.
(iii) G and H are generalized step functions with values (u_0, u_1) and (v_0, v_1) respectively, and D is a generalized delta function. $\square$

Remark 1. The standard choice for a generalized delta function is $D_\varepsilon = \phi_\varepsilon$, $\phi \in \mathcal{A}_0$, i.e. $D = \iota_\phi(\delta)$, where δ is the delta distribution. Also, the standard choice for a representative of a step function is $G = \iota_\phi(g) = g * \phi_\varepsilon/\mathcal{N}_g$, where

$$g = \begin{cases} y_0, & x < 0 \\ y_1, & x > 0 \end{cases} \in L^\infty$$

. The above definition does not provide a unique way to interpret the product of generalized step and delta function (as in [10], where the representatives are chosen in a special way), but this fact has not importance in the case of system (3) as will be shown later.

We shall use the following three lemmas.

Lemma 1. *Let $A \in \mathcal{G}_g(\mathbb{R}^2_+)$ be of a bounded type, $B \geq \tau > 0$, $\tau \in \mathbb{R}$ be a generalized function in $\mathcal{G}_g(\mathbb{R}^2_+)$ and $D \in \mathcal{G}_g(\mathbb{R})$ be a generalized delta function. Then*

$$\frac{A(x,t)}{B(x,t)+s(t)D(x-ct)} \approx \frac{A(x,t)}{B(x,t)}, \tag{6}$$

for any smooth function $s : \mathbb{R}_+ \to \mathbb{R}_+$.

Proof. Take a representatives $B_\varepsilon \geq \tau$ and $D_\varepsilon \geq 0$, $\operatorname{supp} D_\varepsilon \subset [-\varepsilon, \varepsilon]$ of B and D, respectively. Then

$$\begin{aligned} I =& \Big| \iint_{\mathbb{R}^2_+} \Big(\frac{A_\varepsilon(x,t)}{B_\varepsilon(x,t)+s(t)D_\varepsilon(x-ct)} - \frac{A_\varepsilon(x,t)}{B_\varepsilon(x,t)} \Big) \phi(x,t)dxdt \Big| \\ \leq& \iint_{\operatorname{supp}\phi \cap \{(x,t):\ |x-ct|<\varepsilon\}} \Big| \frac{A_\varepsilon(x,t)}{B_\varepsilon(x,t)} \Big| |\phi(x,t)| dxdt. \end{aligned}$$

Since $|A_\varepsilon(x,t)| \leq C_1 < \infty$, the integrand of the last integral is bounded. The fact that $\operatorname{mes}(\operatorname{supp}\phi \cap \{(x,t) :\ |x-ct| < \varepsilon\}) \leq \text{const} \cdot \varepsilon$ proves that $I \to 0$ as $\varepsilon \to 0$. Here mes denotes the Lebesque measure. □

Lemma 2. *Let A, B and D be as above. Let $s_1, s_2 : \mathbb{R}_+ \to \mathbb{R}_+$, $i = 1, 2$, be smooth functions. Then*

$$\frac{A(x,t)s_1(t)D(x-ct)}{B(x,t)+s_2(t)D(x-ct)} \approx 0. \tag{7}$$

Proof. It is easy to see that

$$\Big\| \frac{A_\varepsilon(x,t)s_1(t)D_\varepsilon(x-ct)}{B_\varepsilon(x,t)+s_2(t)D_\varepsilon(x-ct)} \Big\|_{L^\infty(\mathbb{R}^2_+)} = C_\varepsilon < \infty,$$

and

$$\operatorname{mes}\Big(\operatorname{supp}\big(\frac{A_\varepsilon(x,t)s_1(t)D_\varepsilon(x-ct)}{B_\varepsilon(x,t)+s_2(t)D_\varepsilon(x-ct)} \big) \cap \operatorname{supp}\phi \Big) = \mathcal{O}(\varepsilon),\ \varepsilon \to 0,$$

for every $\phi \in C_0^\infty(\mathbb{R}^\infty_+)$. Thus

$$\iint_{\mathbb{R}^2_+} \Big(\frac{A_\varepsilon(x,t)s_1(t)D_\varepsilon(x-ct)}{B_\varepsilon(x,t)+s_2(t)D_\varepsilon(x-ct)} \Big) \phi(x,t)dxdt \to 0,\ \varepsilon \to 0. \square$$

Remark 2. Let us notice that if the generalized delta functions from above have different representatives, the relation (7) might be false . For example, if they have representatives with disjoint supports, then the right-hand-side of (7) will be

$$(A(x,t)/B(x,t))s_1(t)\delta(x-ct)$$

instead of zero.

Lemma 3. *Let A, D and s_i be as above. Suppose that B is of bounded type. Then*

$$\frac{A(x,t)s_1(t)D^2(x-ct)}{B(x,t)+s_2(t)D(x-ct)} \approx A(x,t)\frac{s_1(t)}{s_2(t)}D(x-ct),$$

provided that $s_1(t)/s_2(t)$ can be continuously prolonged to the point $t = 0$.

Proof. Using the fact that $\mathcal{G}_g(\mathbb{R}^2_+)$ is a multiplicative algebra one gets

$$\begin{aligned}
&\frac{A(x,t)s_1(t)D^2(x-ct)}{B(x,t)+s_2(t)D(x-ct)}\\
=&\frac{A(x,t)s_1(t)D^2(x-ct)+A(x,t)\frac{s_1(t)}{s_2(t)}B(x,t)D(x-ct)}{B(x,t)+s_2(t)D(x-ct)}\\
&-\frac{A(x,t)\frac{s_1(t)}{s_2(t)}B(x,t)D(x-ct)}{B(x,t)+s_2(t)D(x-ct)}\\
=&\frac{A(x,t)\frac{s_1(t)}{s_2(t)}D(x-ct)\big(s_2(t)D(x-ct)+B(x,t)\big)}{B(x,t)+s_2(t)D(x-ct)}\\
&-\frac{A(x,t)\frac{s_1(t)}{s_2(t)}B(x,t)D(x-ct)}{B(x,t)+s_2(t)D(x-ct)}\\
\approx&A(x,t)\frac{s_1(t)}{s_2(t)}D(x-ct).
\end{aligned}$$

In the last association process we have used relation (7). □

Now we are in the position to state the following theorem.

Theorem 1. *There exists an overcompressive delta shock wave solution to (3,2) if* $u_l, u_r > 0$, $w_l/u_l > w_r/u_r$.

Proof. Let

$$\begin{aligned}
u(x,t)&=G(x-ct)+s_1(t)D(x-ct)\\
w(x,t)&=H(x-ct)+s_2(t)D(x-ct)
\end{aligned}\tag{8}$$

where G and H are generalized step functions with values (u_l, u_r) and (w_l, w_r), respectively, $s_i : \mathbb{R}_+ \to \mathbb{R}_+$, $s_i(0) = 0$, $i = 1, 2$, are smooth functions, and D is a generalized delta function. In the sequel we shall omit the argument $x - ct$. We have

$$\begin{aligned}
\frac{w^2}{u}&=\frac{(H+s_2(t)D)^2}{G+s_1(t)D}=\frac{H^2+2Hs_2(t)D+s_2^2(t)D^2}{G+s_1(t)D}\\
&=\frac{H^2}{G+s_1(t)D}+\frac{2Hs_2(t)D}{G+s_1(t)D}+\frac{s_2^2(t)D^2}{G+s_1(t)D}\approx\frac{H^2}{G}+0+\frac{s_2^2(t)}{s_1(t)}D,
\end{aligned}\tag{9}$$

by Lemmas 1-3.

Substituting (8) into the first equation of (3) one gets

$$\begin{aligned}
u_t+w_x&\approx -c[G]\delta+s_1'(t)\delta-cs_1(t)\delta'+s_2(t)\delta'+[H]\delta\\
&=(s_1'(t)-c[G]+[H])\delta+(s_2(t)-cs_1(t))\delta'\approx 0.
\end{aligned}$$

Thus, $s_1(t) = \sigma t$, $s_2(t) = c\sigma t$ and

$$\sigma = c[G]-[H].\tag{10}$$

Substitution of (8) into the second equation of (3) and use of (9) yields

$$\begin{aligned} w_t + \Big(\frac{w^2}{u}\Big)_x &\approx -c[H]\delta + s_2'(t)\delta - cs_2(t)\delta' + \Big[\frac{H^2}{G}\Big]\delta + \frac{s_2^2(t)}{s_1(t)}\delta' \\ &= \Big(c\sigma - c[H] + \Big[\frac{H^2}{G}\Big]\Big)\delta + (c^2\sigma - c^2\sigma)\delta' \\ &= \Big(c\sigma - c[H] + \Big[\frac{H^2}{G}\Big]\Big)\delta = 0, \end{aligned}$$

i.e.

$$c(\sigma - [H]) + \Big[\frac{H^2}{G}\Big] = 0. \tag{11}$$

Solving (10) and (11) gives

$$c = \frac{w_r - w_l \pm |w_r/u_r - w_l/u_l|\sqrt{u_l u_r}}{u_r - u_l}.$$

Adding the overcompressiveness condition

$$w_l/u_l \geq c \geq w_r/u_r,$$

one gets the following final result for the speed of the delta shock wave

$$c = \frac{w_r - w_l + (w_l/u_l - w_r/u_r)\sqrt{u_l u_r}}{u_r - u_l},$$

if $[G] \neq 0$, and otherwise

$$c = \frac{w_l + w_r}{2u_r}.$$

In the both cases

$$\sigma = (w_l/u_l - w_r/u_r)\sqrt{u_l u_r}. \tag{12}$$

This proves the theorem. □

Remark 3. (a) Let us notice that the solution obtained in the previous theorem is associated to the distributions

$$\begin{aligned} U(x,t) &\approx \begin{cases} u_l, x < ct \\ u_r, x > ct \end{cases} + \Big(\frac{w_l}{u_l} - \frac{w_r}{u_r}\Big)\sqrt{u_l u_r}\, t\delta(x - ct), \\ W(x,t) &\approx \begin{cases} w_l, x < ct \\ w_r, x > ct \end{cases} + \Big(\frac{w_l}{u_l} - \frac{w_r}{u_r}\Big)\sqrt{u_l u_r}\, ct\delta(x - ct), \end{aligned} \tag{13}$$

where

$$c = \frac{[GH] - [H]\sqrt{u_l u_r}}{[G]} \text{ or } c = \frac{w_l + w_r}{2u_r} \text{ if } [G] = 0.$$

(b) The same limit is obtained in [10] for (1) if one takes $w = uv$ with using singular shock wave solution. But comparing with that one, our solution does not have non-zero correction factors.
(c) Since the value of v on the line $x = ct$ is determined to be c in [1], [5] or [16] the measure-theoretic product uv gives the same solution (13).

3. The numerical algorithm

The algorithm we use here is a modification of the algorithm introduced in [15]. Therefore, we will explain it briefly with a detailed explanation of the changes we made in order to get more efficiency and better resolution. of the particular problem we are interested in.

For a problem of the following form

$$u_t + f(u)_x = 0$$

the procedure is based on two independent parts: a mesh redistribution algorithm and a solution algorithm. We shall first explain the solution algorithm.

Let $\{t_n\}$ denote the sequence of time steps with $\Delta t_n = t_{n+1} - t_n$. Assume that a spatially fixed mesh on the computational domain $[a, b]$ is given by

$$x = x(\xi),\ \xi_j = j/(J+1),\ 0 \le j \le J+1,$$

where $\xi \in [0, 1]$, and

$$x(0) = a \text{ and } x(1) = b.$$

The Godunov scheme (see [8]) assumes that the solution is piecewise constant on each subinterval $[x_j, x_{j+1}]$ and the discrete solution is taken as an average value of the actual solution along the lower cell boundary,

$$U_j^n = \frac{1}{\Delta x_j^n} \int_{x_{j-1/2}}^{x_{j+1/2}} u(x,t)dx,$$

where $\Delta x_j^n = x_{j+1/2}^n - x_{j-1/2}^n$ presents the local spatial step. The method requires the solution of Riemann problems at every cell boundary in each time step. Doing so in practice can be very expensive, especially for nonlinear problems, as is the case with problem (1). Therefore, it is advisable to introduce an approximate Riemann solver. One possibility is the well-known Roe solver, see [13].

The Roe solver is based on the linearized system

$$u_t + \widehat{A} \cdot u_x = 0, \tag{14}$$

where $\widehat{A}$ is an $m \times m$ matrix with the following properties

$$\widehat{A}(u_l, u_r)(u_r - u_l) = f(u_r) - f(u_l), \tag{15}$$

$$\widehat{A}(u_l, u_r) \text{ is diagonizable with real eigenvalues,} \tag{16}$$

$$\widehat{A}(u_l, u_r) \longrightarrow f'(\overline{u}) \text{ when } u_l, u_r \longrightarrow \overline{u}. \tag{17}$$

The Roe linearization will be discussed in details later on. Right now let us assume that the appropriate linearization is available and proceed with solution procedure for the linear problem (14). Notice that (16) implies that $\widehat{A}$ is diagonizable with real eigenvalues, so we can decompose it into

$$\widehat{A} = R\Lambda R^{-1},$$

where $\Lambda = \mathrm{diag}(\lambda_1, \lambda_2, ..., \lambda_m)$ is a diagonal matrix of eigenvalues and $R = [r_1 \mid r_2 \mid ..... \mid r_m]$ is the matrix of the appropriate eigenvectors. Let us introduce the following notation

$$\begin{aligned} \lambda_p^+ &= \max(\lambda_p, 0),\ \Lambda^+ = \mathrm{diag}(\lambda_1^+, ..., \lambda_m^+), \\ \lambda_p^- &= \min(\lambda_p, 0),\ \Lambda^- = \mathrm{diag}(\lambda_1^-, ..., \lambda_m^-), \\ \widehat{A}^+ &= R\Lambda^+R^{-1},\ \widehat{A}^- = R\Lambda^-R^{-1}. \end{aligned}$$

Now, for the linearized system (14) Godunov's method takes the form

$$U_j^{n+1} = U_j^n - \frac{\Delta t_n}{\Delta x_j}\left[\widehat{A}^-(U_{j+1}^n - U_j^n) + \widehat{A}^+(U_j^n - U_{j-1}^n)\right]. \tag{18}$$

Besides that, the scheme requires the time step to satisfy the Courant-Friedrichs-Levy stability condition [9],

$$\nu = \max_{j,p}\left|\frac{\Delta t_n}{\Delta x_j}\lambda_p(U_j^n)\right| \le 1. \tag{19}$$

Although, in practice a more restrictive condition $\nu \le 0.9$ is used. It is also important to mention that the Godunov scheme is implemented in the software package CLAWPACK ([7]) and we used this implementation.

Let us finally discuss the Roe linearization procedure determined by (15) - (17). The condition (15) is reflecting R-H discontinuity condition in the solution. From (16) we get that the system is hyperbolic and solvable and (17) imply consistency with the original nonlinear system. In order to get an appropriate

$$u_t + \widehat{A}u_x = 0.$$

we start with condition (15) and get the equation

$$\begin{bmatrix} \alpha & \beta \\ \gamma & \delta \end{bmatrix} \cdot \begin{bmatrix} u_r - u_r \\ w_r - w_l \end{bmatrix} = \begin{bmatrix} w_r - w_l \\ \frac{w_r^2}{u_r} - \frac{w_l^2}{u_l} \end{bmatrix}.$$

Starting from this equation and using condition (17) we get the matrix $\widehat{A}$,

$$\widehat{A} = \begin{bmatrix} 0 & 1 \\ -\dfrac{w_r w_l}{u_l u_r} & \dfrac{w_r}{u_r} + \dfrac{w_l}{u_l} \end{bmatrix}.$$

Clearly, conditions (15) and (17) are satisfied. The eigenvalues of $\widehat{A}$ are

$$\lambda_{1,2} = \frac{1}{2}\left(\frac{w_r}{u_r} + \frac{w_l}{u_l} \pm \left|\frac{w_r}{u_r} - \frac{w_l}{u_l}\right|\right)$$

and the corresponding eigenvectors

$$r_1 = \begin{bmatrix} 1 \\ \lambda_1 \end{bmatrix} \text{ and } r_2 = \begin{bmatrix} 1 \\ \lambda_2 \end{bmatrix}.$$

The system (3) we considered in our paper is weakly hiperbolic, i.e. the two eigenvalues λ_1 and are λ_2 the same. One typical approach to fix the lack of hiperbolicity is to add an pertubation term to the system (See section 4.2), in order to get a hyperbolic system. Therefore we will consider two cases: $\lambda_1 \neq \lambda_2$ for the system with perturbation and $\lambda_1 = \lambda_2$ for the weakly hyperbolic case - the system without perturbation. Since the solution to a Riemann problem of a linear hyperbolic system of PDE's consists of jumps of the form

$$[U] = \sum_p \alpha_p r_p,$$

see [8], we have

$$\begin{aligned} \begin{bmatrix} u_r - u_l \\ w_r - w_l \end{bmatrix} =& \alpha_1 r_1 + \alpha_2 r_2 \\ =& \alpha_1 \begin{bmatrix} 1 \\ \lambda_1 \end{bmatrix} + \alpha_2 \begin{bmatrix} 1 \\ \lambda_2 \end{bmatrix}. \end{aligned} \tag{20}$$

If $\lambda_1 \neq \lambda_2$ relation (20) yields

$$\begin{aligned} u_r - u_l =& \alpha_1 + \alpha_2 \\ w_r - w_l =& \alpha_1 \lambda_1 + \alpha_2 \lambda_2, \end{aligned}$$

so we have

$$(\alpha_1, \alpha_2) = \left(\frac{w_r - w_l + \lambda_2(u_l - u_r)}{\lambda_1 - \lambda_2}, \frac{w_l - w_r + \lambda_1(u_r - u_l)}{\lambda_1 - \lambda_2} \right).$$

Let us now explain how to handle weakly hyperbolic system (3) without perturbation. Since we have $\lambda_1 = \lambda_2$, there holds $r_1 = r_2$, and (20) gives

$$\begin{aligned} u_r - u_l =& \alpha_1 + \alpha_2 \\ w_r - w_l =& (\alpha_1 + \alpha_2)\lambda_1. \end{aligned}$$

One of possible solutions of the above system is

$$(\alpha_1, \alpha_2) = (0, u_r - u_l)$$

and therefore the weak hyperbolic system is also solvable. Thus we have shown that the Roe linearization exists in both cases.

Let us now explain the mesh redistribution algorithm.

The equidistribution principle (a detailed explanation can be found in [6]) is formulated as $Mx_\xi =$ constant or equivalently

$$(Mx_\xi)_\xi = 0 \tag{21}$$

for a monitor function $M(x, y) > 0$. Generally speaking, the monitor function is an appropriately chosen measure of numerical solution of the physical PDE. In order to solve the mesh redistribution equation (21), in [15] it is suggested to take an artificial time τ and solve

$$x_\tau = (Mx_\xi)_\xi, \ 0 < \xi < 1 \tag{22}$$

with boundary conditions $x(0, \tau) = a$ and $x(1, \tau) = b$. Making discretization of (22) we get

$$\widetilde{x}_j = x_j + \frac{\Delta\tau}{\Delta\xi^2}[M_j(x_{j+1} - x_j) - M_{j-1}(x_j - x_{j-1})], \tag{23}$$

where $\Delta\xi = 1/(J+1)$. Solving (23) with boundary conditions $x_0 = a$ and $x_{J+1} = b$ leads to a new grid.

In [15] it is also suggested to use the following Gauss-Seidel type iteration to solve the mesh moving equation (21):

$$M_j^n(x_{j+1}^n - x_j^{n+1}) - M_{j-1}^n(x_j^{n+1} - x_{j-1}^{n+1}) = 0. \tag{24}$$

In the above mentioned paper it is demonstrated that the new mesh $\{x^{n+1}\}$ generated by (24) keeps the monotonic order of $\{x^n\}$.

n this paper, we will introduce an alternative approach. We will use a Newton-type iteration to solve (21):

$$M_j(x_{j+1}^{n+1} - x_j^{n+1}) - M_{j-1}(x_j^{n+1} - x_{j-1}^{n+1}) = 0. \tag{25}$$

Let us demonstrate that the new mesh $\{x^{n+1}\}$ generated by (24) keeps the monotonic order of mesh points $\{x^n\}$.

Lemma 4. *Assume $x_j^n > x_{j-1}^n$, for $1 \le j \le J$. If the new mesh $\{x^{n+1}\}$ is obtained by using Newton's iterative scheme for (23), then $x_j^{n+1} > x_{j-1}^{n+1}$, for $1 \le j \le J$.*

Proof. From (23) we have

$$M_j x_{j+1}^{n+1} - (M_j + M_{j-1})x_j^{n+1} + M_{j-1}x_{j-1}^{n+1} = 0,$$

which gives

$$-\alpha_j x_{j+1}^{n+1} + x_j^{n+1} - \beta_j x_{j-1}^{n+1} = 0, \tag{26}$$

after dividing by $-(M_j + M_{j-1})$. Here

$$\alpha_j = \frac{M_j}{M_j + M_{j-1}} \text{ and } \beta_j = \frac{M_{j-1}}{M_j + M_{j-1}}.$$

Obviously, $\alpha_j, \beta_j > 0$. Since $\alpha_j + \beta_j = 1$, equation (26) yields

$$(\beta_j - 1)x_{j+1}^{n+1} + x_j^{n+1} \pm \beta_j x_j^{n+1} - \beta_j x_{j-1}^{n+1} = 0,$$

which implies

$$(x_j^{n+1} - x_{j+1}^{n+1}) - \beta_j(x_{j-1}^{n+1} - x_j^{n+1}) = \beta_j(x_j^{n+1} - x_{j+1}^{n+1}),$$

i.e.

$$(x_j^{n+1} - x_{j+1}^{n+1}) - \beta_j(x_{j-1}^{n+1} - x_j^{n+1}) = (1-\alpha_j)\beta_j(x_j^{n+1} - x_{j+1}^{n+1}),$$

which gives

$$(x_j^{n+1} - x_{j+1}^{n+1}) - (1-\alpha_j)(x_j^{n+1} - x_{j+1}^{n+1}) = \beta_j(x_{j-1}^{n+1} - x_j^{n+1}),$$

i.e.

$$\alpha_j(x_j^{n+1} - x_{j+1}^{n+1}) = \beta_j(x_{j-1}^{n+1} - x_j^{n+1}). \tag{27}$$

Suppose

$$x_{j-1}^{n+1} > x_j^{n+1}, \text{ i.e. } x_{j-1}^{n+1} - x_j^{n+1} > 0 \tag{28}$$

for some j, $1 < j < J$. Relations (27), (28) and positivity of α_j and β_j yields

$$x_j^{n+1} - x_{j+1}^{n+1} > 0, \text{ i.e. } x_j^{n+1} > x_{j+1}^{n+1}.$$

Continuing in such a way we get

$$a = x_0^{n+1} > ... > x_{j-1}^{n+1} > x_j^{n+1} > x_{j+1}^{n+1} > ... > x_J^{n+1} = b,$$

which is impossible. Therefore, $x_j^{n+1} < x_{j+1}^{n+1}$ for all j, $1 \le j \le J$. □

Few remarks about the monitor function M are due here. If M is the arc-length function, i.e.

$$M = \sqrt{1 + |u_x|^2},$$

then the corresponding centered finite difference approximation is given by

$$M_j = \sqrt{1 + \left|\frac{\overline{U}_{j+1} + \overline{U}_j}{x_{j+1} - x_j}\right|},$$

where

$$\overline{U}_j = (U_{j+1}\Delta x_j + U_j \Delta x_{j+1})/(\Delta x_{j+1} + \Delta x_j).$$

As M is largest where the solution changes most rapidly, the spatial points concentrate in regions with large gradient changes. In order to avoid local oscillation due to the large gradient changes, it is useful to replace the mesh function with a regularized version $\widetilde{M}_i$. The regularized function we use in this paper is suggested in [15] and is given by

$$\widetilde{M}_j \approx \frac{1}{4}(M_{j+1} + 2M_j + M_{j-1}). \tag{29}$$

Using (25) and (29) we get

$$\widetilde{M}_j^{n,m} x_{j+1}^{n,m+1} - (\widetilde{M}_j^{n,m} + \widetilde{M}_{j-1}^{n,m}) x_j^{n,m+1} + \widetilde{M}_{j-1}^{n,m} x_{j-1}^{n,m+1} = 0. \tag{30}$$

To balance the number of points inside a steep internal layer, we use a regularizing factor α in the following manner:

$$M = \sqrt{1 + \frac{1}{\alpha}|u_x|^2},$$

where $\alpha > 1$. The factor α allows us to reduce the magnitude of the monitor function in situations where $|u_x|$ is very large, thereby avoiding over-resolution of steep layers, while also ensuring that M still retains a significant peak near these discontinuities. Different approaches in scaling α, based on the maximum solution value, maximum derivative value or the average value of the derivative over the spatial domain, suggested in [4], [8] and [14] respectively, have been successful with linearized mesh equation, but do not behave well in nonlinear case. Therefore, in [15] the regularizing factor is suggested to be taken for free. However, in the region where the monitor function has high magnitude, there is a significant number of points, so Δx_j goes to zero. Thus, in some time step, while moving the mesh from $\{x_j^{n,m}\}$ to $\{x_j^{n,m+1}\}$ the CFL number (19) can go out of the feasible range (i.e. $\nu > 0.9$). So one has to interrupt the moving mesh procedure by taking the previous mesh $\{x_j^{n,m}\}$, although $\|x_j^{n,m} - x_j^{n,m-1}\| > \varepsilon$. In order to avoid such interruption of the numerical procedure if $\nu > 0.9$, we suggest increasing the regularizing factor with some fixed amount and performing the current time step again.

Since the shock travel within spatial domain with time it is necessary to generate mesh that is also moving within spatial domain. Otherwise we would not be able to follow the solution for longer time intervals. This mesh adjustment is done using the following procedure. The current spatial domain is divided into two parts according to the position of the maximum of the numerical solution. If the interval on the left side of the maximum is longer than the right one, the first point from the left interval is catted and a new point is added to the end of the other interval. The procedure is to be repeated until the two intervals are of equal length.

Using the algorithm proposed in [15] with the modifications explained above we get the following numerical procedure.

Algorithm.

Step 1: Given an initial solution U^0 at time $t = t^0$, equidistribute the mesh exactly using a discretization of the exact equidistribution principle $(Mx)_\xi = 0$. Given an initial value α^*, set $\alpha = \alpha^*$.

Step 2: Increase the time level to $t = t^{n+1}$ and take a guess at the new mesh positions using $\left\{x_j^{n+1,0}\right\} = \left\{x_j^n\right\}$ and move grid from $\left\{x_j^{n+1,m}\right\}$ to $\left\{x_j^{n+1,m+1}\right\}$ using (30) and compute $\left\{U_j^{n+1,m+1}\right\}$on the new grid based on the Godunov scheme (18) with $\nu \leq 0.9$. If $\nu > 0.9$, go set $\alpha := \alpha + 10$ and go to the beginning of Step 2. Repeat the updating procedure until $\left\|x^{n+1,m+1} - x^{n+1,m}\right\| \leq \varepsilon$.

Step 3: Compute $\left\{U_j^{n+1}\right\}$ on the new mesh $\left\{x_j^{n+1}\right\}$ obtained in the pervious step to get the solution approximations at time level t_{n+1}.

Step 4: Adjust the mesh such that the position of the maximizer (spatial point for which the current approximation has maximal value) is approximately the middle mesh point.

Step 5: If $t_{n+1} \leq T$, go to step 2.

4. Application to the solutions with singular shock

4.1. **Pressureless system.** Denote with u_s and w_s the singular parts of the delta shock wave (5), i.e.

$$\begin{aligned} u_s(x,t) =& s_1(t)D(x-ct) \\ w_s(x,t) =& s_2(t)D(x-ct), \end{aligned}$$

and set

$$Q(t) := \int U_s(x,t)dx \text{ and } P(t) := \int W_s(x,t)dx,\ t > 0.$$

Clearly, Q and P represent the surfaces below the non-constant parts of the solution components. The definition of delta function implies $\int Ddx \approx 1$, so $Q \approx s_1(t)$. By (12) and (13) one gets

$$Q \approx \sigma t \approx \left(\frac{w_l}{u_l} - \frac{w_r}{u_r}\right)\sqrt{u_l u_r}t, \tag{31}$$

$$P \approx c\sigma t \approx c\left(\frac{w_l}{u_l} - \frac{w_r}{u_r}\right)\sqrt{u_l u_r}t. \tag{32}$$

From (31) and (32) there follows that both P and Q are linearly time dependent, so their ratio is constant, i.e. $P/Q = c$.

4.2. **Perturbation by a hyperbolic system.** Consider now the isentropic (p-system) gas dynamics system

$$\begin{aligned} u_t + (uv)_x &= 0 \\ (uv)_t + (uv^2 + \mu p(u))_x &= 0 \end{aligned}$$

with the initial data

$$u(x,0) = \begin{cases} u_l, & x < 0 \\ u_r, & x > 0 \end{cases}, v(x,0) = \begin{cases} v_l, & x < 0 \\ v_r, & x > 0 \end{cases},$$

where $p(u) = \mu u^\gamma$, $\gamma \in (1,3)$.

One can take $\mu = (\gamma-1)^2/(4\gamma)$ and letting $\mu \to 0$ we have $\gamma \to 1$ what is a physical constitution law, see page 253 of [3]. In numerical tests we shall consider the following cases:

(1) $\gamma = \frac{5}{3}$ - approach adopted by [15],
(2) $\gamma = \gamma(\mu)$,
(3) $\mu = 0$.

Obviously $\gamma = 5/3$ is more simple than $\gamma = \gamma(\mu)$ but if $\gamma = 5/3$ then the velocity c is zero and thus one gets the wave without spatial movements. Also $\mu = 0$ implies that there is no change in original system, while the perturbation (2) introduced in this paper has physical meaning and leads to relievable results for decent time intervals as will be shown here.

Since we are doing the case when the vacuum state does not appear, it is possible to look at the system after the change of variables $uv \mapsto w$,

$$u_t + (w)_x = 0$$
$$w_t + (w^2/u + \mu p(u))_x = 0$$

with new initial data

$$u(x,0) = \begin{cases} u_l, \ x < 0 \\ u_r, \ x > 0 \end{cases}, w(x,0) = \begin{cases} w_l = u_l v_l, x < 0 \\ w_r = u_r v_r, x > 0 \end{cases},$$

where $w_l/u_l > w_r/u_r$.

The isentropic system is strictly hyperbolic with both of the fields being genuinely nonlinear. The shock curves are given by

$$S_i: \ w_r - w_l = \frac{w_l}{u_l}(u_r - u_l) + (-1)^i \sqrt{\frac{u_r}{u_l} \frac{\mu u_r^\gamma - \mu u_l^\gamma}{u_r - u_l}}(u_r - u_l)$$
$$(-1)^i(u_r - u_l) < 0, \ u_l, u_r > 0.$$

In [1], the authors proved that for each pair (u_l, w_l), (u_r, w_r) such that $w_l/u_l > w_r/u_r$, solution consists of two shock waves, and this solution tends to a delta shock wave as $\mu \to 0$. The obtained delta shock wave in the limit is the same as the one solving pressureless system (when $\mu = 0$). With the same arguments as in that article, one can prove that this stays true for renormalized γ. These facts are verified numerically here for pressureless system.

5. Numerical Results

Let us now consider the system (3) with the initial data (2). Since the initial conditions are discontinuous, the selection of an appropriate initial mesh is of particular importance. In order to allow mesh points to concentrate on or near the initial discontinuities, the data must be smoothed over some finite width. We therefore replace (2) with a smoothed function of the form

$$\widetilde{U}(x) = U_l + \frac{1}{2}(U_r - U_l)\left(1 + \tanh\left(\frac{x}{\varepsilon}\right)\right),$$

where $U_l = (u_l, w_l)$, $U_r = (u_r, w_r)$ and $\varepsilon = 0.005$ as the smoothing width.

The description of parameters used in our examples can be found in Table 1.

Parameter	Description
t	time
$[x_1, x_2]$	spatial domain
J	number of mesh points
α^*	initial value of the regularizing factor
α	final value of the regularizing factor obtained by the program
μ	perturbation coefficient tending to zero
γ	$\in (1,3)$ is fixed or depending on μ

Table 1. The description of parameters used in our examples

We use the following data for numerical examples.

$$U_l = (1, 0.2),\ U_r = (1.2, 0.2),\ \frac{x_2 - x_1}{J} = \frac{1}{20},\ \alpha^* = 10.$$

We compare the results obtained without and with perturbation by the isentropic system. In the later case we take $\mu \in \{0.01, 0.001, 0.0001\}$, $\gamma = 2\mu + 2\sqrt{\mu + \mu^2}$ and $\gamma = \frac{5}{3}$. Theorem 1 gives the predicted speed $c = 0.18257$ and mass quotient $P/Q = 0.18257$. Also one can easily check that both of P and Q are linearly time dependent.

The results are the summarized in the following tables.

	P	Q	P/Q
$t_1 = 12.1435$	0.07693	0.42481	0.18110
$t_2 = 24.0287$	0.15087	0.83043	0.18168
$t_3 = 36.0157$	0.22886	1.25012	0.18307
$t_4 = 48.1054$	0.30914	1.68753	0.18319
$t_5 = 60.136$	0.38428	2.10093	0.18291

TABLE 2. System without perturbation, $\mu = 0$

	P	Q	P/Q	c_l	c_r
$t_1 = 6.1106$	0.01911	0.14452	0.13209	0.04909	0.29457
$t_2 = 12.0250$	0.03751	0.23418	0.16017	0.04158	0.29106
$t_3 = 18.0682$	0.05633	0.31383	0.17948	0.04981	0.30440
$t_4 = 24.1149$	0.07515	0.39349	0.19099	0.05805	0.31101
$t_5 = 30.0423$	0.09361	0.49316	0.18982	0.05325	0.31289

TABLE 3. $\gamma = 5/3$, $\mu = 0.01$

	P	Q	P/Q	c_l	c_r
$t_1 = 20.0015$	0.12631	0.71752	0.17603	0.14000	0.2200
$t_2 = 40.0338$	0.25264	1.37278	0.18403	0.14488	0.22231
$t_3 = 60.0916$	0.37906	2.02281	0.18690	0.14145	0.2230
$t_4 = 80.1589$	0.50549	2.71331	0.18630	0.14346	0.22081
$t_5 = 100.0650$	0.63087	3.41852	0.18455	0.14490	0.21986

TABLE 4. $\gamma = 5/3$, $\mu = 0.001$

	P	Q	P/Q	c_l	c_r
$t_1 = 60.1454$	0.39319	2.14957	0.18292	0.17458	0.19785
$t_2 = 120.021$	0.78106	4.24315	0.18408	0.17663	0.19580
$t_3 = 180.134$	1.16688	6.36874	0.18322	0.17598	0.19707
$t_4 = 240.068$	1.55000	8.51507	0.18199	0.17745	0.19619
$t_5 = 300.183$	1.93262	10.6857	0.18086	0.17656	0.19655

TABLE 5. $\gamma = 5/3$, $\mu = 0.0001$

	P	Q	P/Q	c_l	c_r
$t_1 = 6.0973$	0.02554	0.19425	0.13146	0.07380	0.27881
$t_2 = 12.0013$	0.05016	0.31376	0.15987	0.07499	0.27070
$t_3 = 18.0444$	0.07454	0.43330	0.17394	0.07759	0.27709
$t_4 = 24.0924$	0.10059	0.54286	0.18530	0.07471	0.27394
$t_5 = 30.0142$	0.12529	0.65243	0.19203	0.07663	0.27987

TABLE 6. $\gamma = 2\mu + 2\sqrt{\mu + \mu^2}$, $\mu = 0.01$

	P	Q	P/Q	c_l	c_r
$t_1 = 20.0051$	0.12887	0.73363	0.17567	0.15496	0.20495
$t_2 = 40.0855$	0.25841	1.43772	0.17973	0.15467	0.20955
$t_3 = 60.0263$	0.38695	2.12212	0.18234	0.15493	0.20658
$t_4 = 80.1492$	0.51660	2.80646	0.18407	0.15721	0.20587
$t_5 = 100.103$	0.64511	3.49079	0.18480	0.15884	0.20878

TABLE 7. $\gamma = 2\mu + 2\sqrt{\mu + \mu^2}$, $\mu = 0.001$

	P	Q	P/Q	c_l	c_r
$t_1 = 100.148$	0.64534	3.53227	0.18270	0.18073	0.19172
$t_2 = 200.071$	1.25455	6.83558	0.18353	0.18093	0.19143
$t_3 = 300.024$	1.84601	10.0449	0.18378	0.18165	0.19165
$t_4 = 400.021$	2.42775	13.2112	0.18376	0.18174	0.19124
$t_5 = 500.026$	3.00301	16.3527	0.18364	0.18179	0.19099

TABLE 8. $\gamma = 2\mu + 2\sqrt{\mu + \mu^2}$, $\mu = 0.0001$

It is quite obvious from the presented tables that the perturbation parameter μ allows computation of an approximate solution for quite long time intervals. In fact the results in Table 1 obtained without perturbation with the described numerical procedure are good but we are unable to follow the solution after $T \approx 60$. This is obviously better than the time reported in [1] and we believe that this fact is a consequence of numerical procedure used in this paper.

All other tables are obtained with perturbation parameter and clearly indicate the ability of numerical procedure to follow the approximate solution for quite a long time. Also smaller μ implies larger T. Since the main idea in numerical method was to confirm theoretical expectation that perturbation of weakly hyperbolic system into strictly hyperbolic implies existence of delta shock, larger T is certainly desirable property. Couple of differences that are noticeable from Tables 2-8 favors the use of $\gamma(\mu)$. For $\gamma = 5/3$ there is a slight decrease in P/Q after some time. We think that such decrease is a consequence of error accumulation. Such effect does not exist when we use $\gamma(\mu)$. Further more $\gamma(\mu)$ has physical meaning since small μ implies that pressure goes to zero and the original problem is pressureless, [3]. Additional quality of numerical approximation with $\gamma(\mu)$ is that the difference between c_1 and c_2 is smaller than the difference obtained for $\gamma = 5/3$.

Figures 1 and 2 show the difference between approximate solution without and with perturbation parameter. The first two pictures show functions u and w at final T. Three dimensional pictures are given in the second row while the third row contains P/Q. In both cases we have clearly formed delta shocks, with greater width in Figure 2 as expected. Mass quotients for both perturbations, $\gamma = 5/3$ and $\gamma = \gamma(\mu)$ are compared on Figure 3. In all cases we are approaching the theoretical value but smaller μ implies better behavior. As a conclusion we can state that the applied numerical procedure successfully deals with this kind of problems and the obtained numerical results are in concordance with theoretical expectations.

References

[1] Chen, G-Q., Liu, H, *Formation of δ-shocks and vacuum states in the vanishing pressure limit of solutions to the Euler equations for isentropic fluids*, SIAM J. Math. Anal. 34 (2003), 925-938.

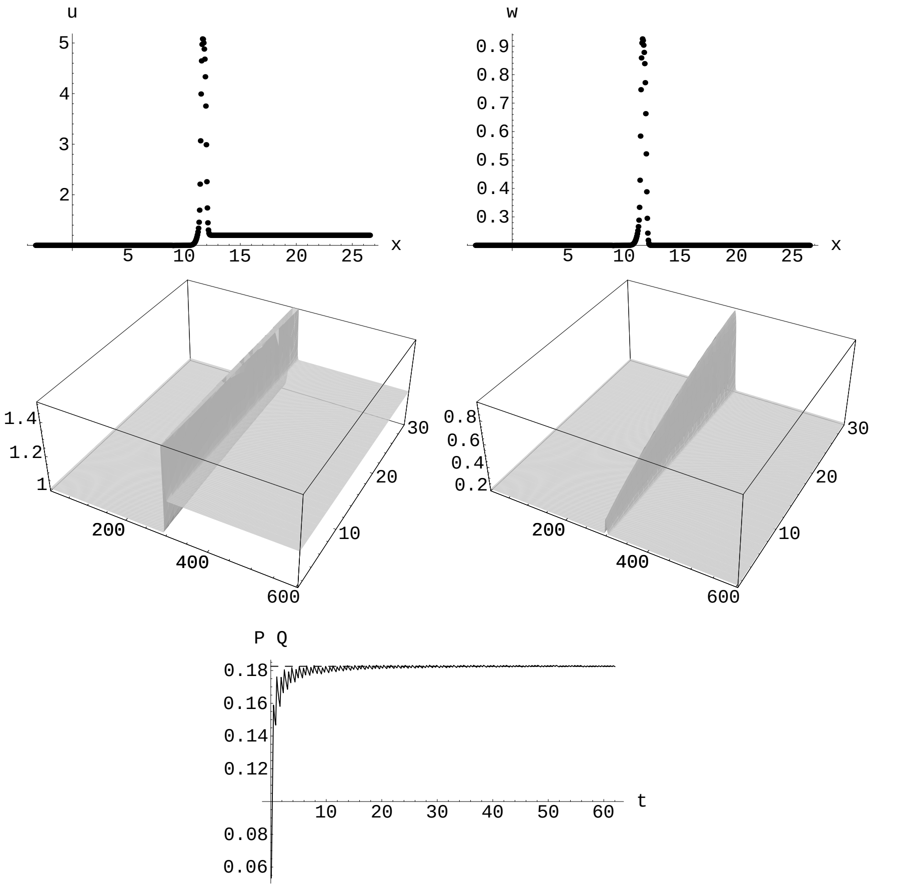

FIGURE 1. The system without perturbation

[2] Colombeau, J.F., Multiplication of Distributions, Lecture Notes in Mathematics 1532, Springer, 1992.

[3] Dafermos, C.M., Hyperbolic Conservation Laws in Continuum Physics, Springer, 2005.

[4] Dorfi, E.A., Drury, L.O., *Simple adaptive grids for 1-D initial value problems*, J. Comput. Phys. 69 (1987).

[5] Huang F., *Weak solutions to pressureless type system*, Comm. PDEs (2005).

[6] Huang W., Ren Y., Russell R.D., *Moving mesh partial differential equations (MMPDES) based on the equidistribution principle*, Siam J. Numer. Anal. 31,3 (1994).

[7] Le Veque, R.J., *Clawpack software,* http://www.amath.washington.edu/~rjl/ clawpack.html.

[8] LeVeque, R. J., *Numerical methods of conservation laws*, ETH Zürich, Basel, (1990).

[9] LeVeque, R.J., Temple, B., *Stability of Godunov's method for a class 2×2 systems of conservation laws*, Trans. Amer. Math. Soc. 288, 1985.

[10] Nedeljkov, M., *Delta and singular delta locus for one dimensional systems of conservation laws*, Math. Meth. Appl. Sci. 27 (2004), 931-955.

[11] Oberguggenberger, M., Multiplication of Distributions and Applications to Partial Differential Equations, Pitman Res. Not. Math. 259, Longman Sci. Techn., Essex, 1992.

[12] Oberguggenberger, M. and Wang, Y-G., *Generalized solutions to conservation laws*, Zeitschr. Anal. Anw. 13(1994), 7-18.

[13] Roe, P.L., *Approximate Riemann solvers, parameter vectors and difference schemes*, J. Comput. Phys., 43 (1981).

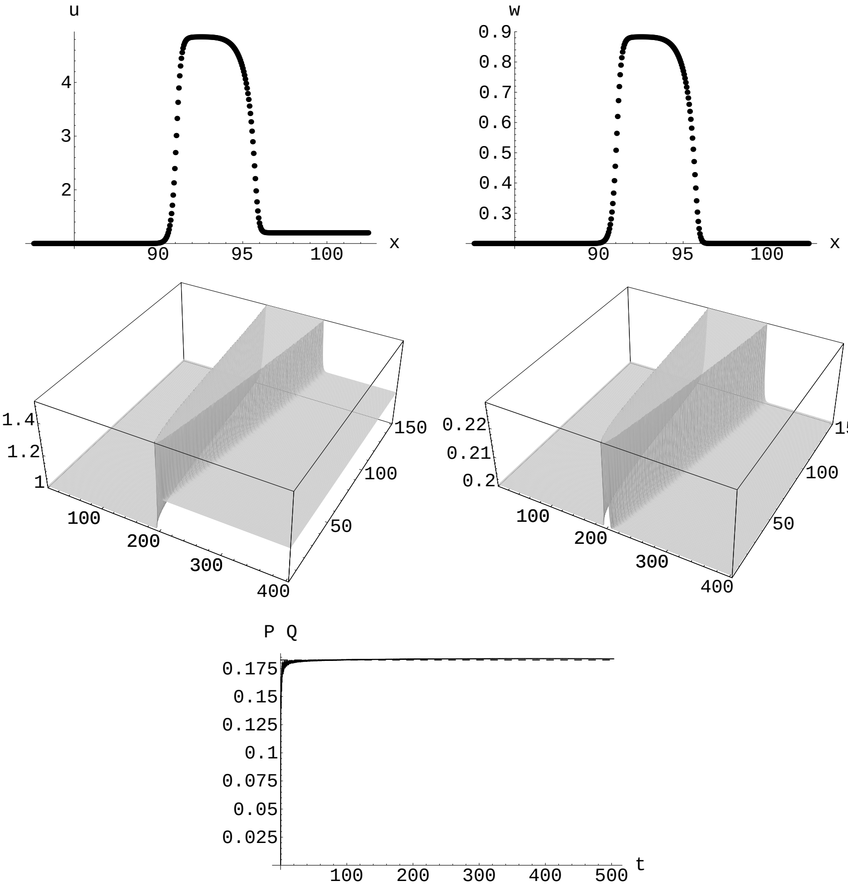

FIGURE 2. $\gamma = 2\mu + 2\sqrt{\mu + \mu^2}$, $\mu = 0.0001$

[14] Stockie, J. M., Mackenzie, J. A., Russell, R. D., *A moving mesh method for one-dimensional hyperbolic conservation laws,* http://www.siam.org/journals7sisc/22-5/36422.html, (2001).

[15] Tang, H., Tang, T., *Adaptive mesh methods for one- and two-dimensional hyperbolic conservation laws,* Peking, Hong Kong.

[16] Yang, H., *Riemann problems for a class of coupled hyperbolic systems of conservation laws*, J. Diff. Eq. 159 (1999), 447-484.

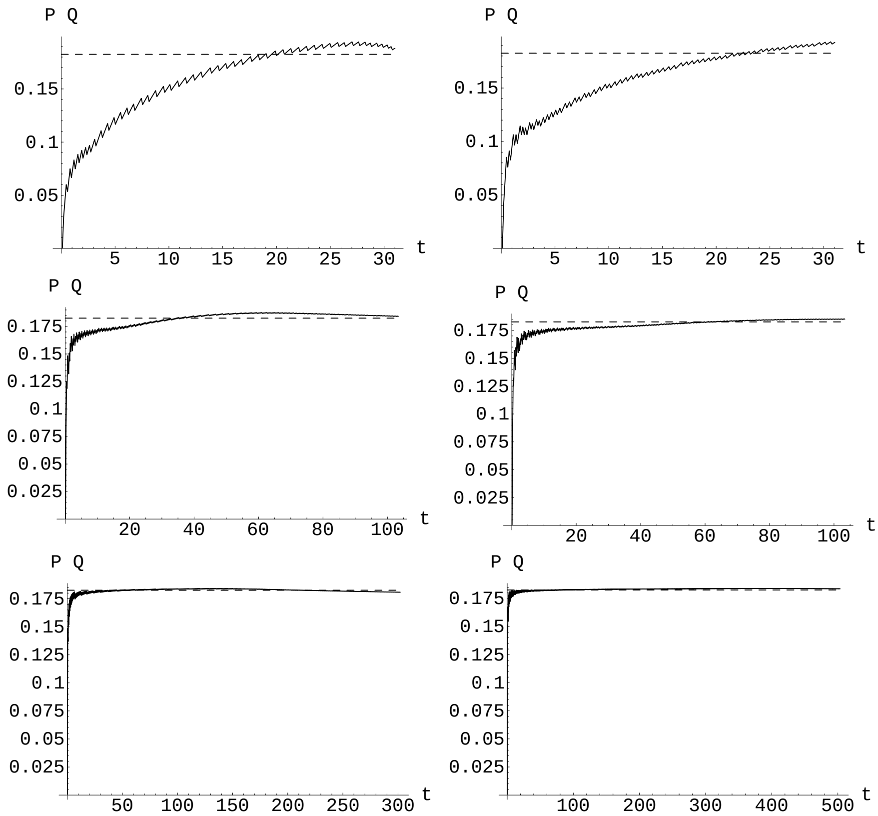

FIGURE 3. Mass quotients: left column – $\gamma = 5/3$, right column – $\gamma = 2\mu + 2\sqrt{\mu + \mu^2}$, μ decreasing from above